Int. J. Heat Mass Transfer. Vol. 12, pp. 1295–1309. Pergamon Press 1969. Printed in Great Britain

AN ANALYSIS OF LAMINAR COMBINED FORCED AND FREE CONVECTION HEAT TRANSFER IN A HORIZONTAL TUBE

G. N. FARIS† and R. VISKANTA

School of Mechanical Engineering, Purdue University, Lafayette, Indiana 47907, U.S.A.

(*Received* 12 *June* 1968 *and in revised form* 20 *February* 1969)

Abstract—An analysis of combined forced and free convection heat transfer of a quasi-incompressible fluid flowing laminarly in a horizontal tube is presented. The physical properties are assumed to be independent of temperature and the heat flux imposed at the tube wall is considered to be uniform along the tube and around the circumference. The flow and heat transfer are specialized for fully developed conditions and the resulting partial differential equations are solved by a perturbation method. Approximate analytical solutions as well as average Nusselt numbers are presented graphically for a range of Prandtl and Grashof numbers of physical interest. The predicted velocity, temperature and average Nusselt numbers are compared with available experimental data.

NOMENCLATURE

A, characteristic velocity, $\sqrt{(gR_i/\varepsilon)}$;
B_i, body force;
c_p, specific heat at constant pressure;
D, pipe diameter;
F, dimensionless parameter, GrE/Re^2;
g, acceleration due to gravity;
g_Z, g_r, g_ϕ, components of acceleration due to gravity in the Z, r, and ϕ directions;
Gr, Grashof number, $\beta g(T_w - T_m)R_i^3/\nu^2$;
Gr_Z, Grashof number based on axial temperature gradient, $\beta g R_i^4(\mathrm{d}T_m/\mathrm{d}Z)/\nu^2$;
$\bar{h}$, average heat transfer coefficient for fully developed flow based on wall to bulk temperature difference;
$h(\phi)$, local (circumferential) heat transfer coefficient for fully developed flow based on wall to bulk temperature difference;
k, thermal conductivity;
L, length of heated section;
$\overline{Nu}$, average Nusselt number, $\bar{h}R_i/k$;
$Nu(\phi)$, local (circumferential) Nusselt number, $h(\phi)R_i/k$;
Nu_0, Nusselt number for pure forced convection;
P, molecular pressure;
p, dimensionless pressure, $P/\rho W_m^2$;
Pe, Peclet number, $RePr$;
Pr, Prandtl number, $\mu c_p/k$;
q'', average wall heat flux;
Ra, Rayleigh number $PrGr_Z$;
R, pipe radius;
r, radial distance measured from centerline of the tube;
Re, Reynolds number, $W_m R_i/\nu$;
T, temperature of fluid;
U, radial fluid velocity;
u, dimensionless radial velocity, $U/A\varepsilon$;
V, angular fluid velocity;
v, dimensionless angular velocity, $V/A\varepsilon$;
W, axial fluid velocity;
w, dimensionless axial velocity, W/W_m;
Z, axial coordinate;
z, dimensionless axial distance, Z/L.

† Present address: IBM Components Division, Endicott, New York.

Greek symbols

α, thermal diffusivity;

β, volumetric coefficient of thermal expansion;

Γ, dimensionless parameter, $PeGr_Z/\sqrt{(Re)}$;

γ, dimensionless group, $\gamma = R_i^2 \frac{\partial P}{\partial Z} \Big/ \mu W_m$;

∇^2, Laplacian in cylindrical coordinates $\nabla^2 \equiv \frac{\partial}{\partial \eta^2} + \frac{1}{\eta}\frac{\partial}{\partial \eta} + \frac{1}{\eta^2}\frac{\partial^2}{\partial \phi^2}$;

∇^4, Laplacian of Laplacian in cylindrical coordinates

$$\nabla^4 \equiv \frac{\partial^4}{\partial \eta^4} + \frac{2}{\eta}\frac{\partial^3}{\partial \eta^3} - \frac{1}{\eta^2}\frac{\partial^2}{\partial \eta^2} + \frac{1}{\eta^3}\frac{\partial}{\partial \eta} + \frac{2}{\eta^2}\frac{\partial^4}{\partial \phi^2 \partial \eta^2} - \frac{2}{\eta^3}\frac{\partial^3}{\partial \phi^2 \partial \eta};$$

ε, dimensionless parameter defined by $\varepsilon = \beta(T_w - T_m)$;

η, dimensionless radial coordinate, r/R_i;

θ, dimensionless temperature, $(T_m - T)/(T_w - T_m)$;

μ, dynamic viscosity;

ν, kinematic viscosity

ρ, density;

ϕ, polar angle measured from top point of tube circumference;

$\dot{\Phi}$, dissipation function;

Ψ, dimensionless stream function.

Subscripts

0, 1, 2, refers to zero, first, and second-order approximations;

c, refers to centerline;

D, refers to diameter;

f, refers to fluid;

i, refers to the inside of the tube wall;

m, refers to mixing cup (bulk) temperature.

1. INTRODUCTION

PURE forced convective heat transfer seldom occurs in reality since the density of ordinary fluids is dependent on temperature. In fact, mixed convection, that is, combined free and forced convection, is the most general type of phenomena. Pure forced or pure free convection are only the limiting cases when either type of mixing motion can be neglected in comparison to the other.

In many practical applications where both free and forced convection effects are of comparable order of magnitude, an indication of the relative magnitude of the two effects may be obtained from a study of the nondimensional parameters appearing in the governing conservation equations of the fluid flow and energy. Still, some situations are encountered where a clear distinction between the two types of motion is difficult to make. This results in a somewhat arbitrary designation of the governing convective heat transfer phenomena. Metais [1] has arbitrarily considered mixed convection to occur when the calculated heat transfer coefficient is ten per cent higher than the corresponding heat transfer coefficient for either pure free or pure forced convection situations.

For pure forced convection analysis and experiment covering the thermally developed and the thermally developing regions have received considerable attention. When natural convection effects are pronounced the orientation of the tube axis becomes important, the two limiting alignments being vertical and horizontal. In vertical tubes the velocities due to buoyancy forces are parallel to the direction of the forced motion; thus, rotational symmetry is retained, and it is possible to solve analytically the equations of motion and energy even in the case of mixed convection. However, in the case of horizontal tubes, the buoyancy and pressure forces in combined free and forced convection are perpendicular to each other, resulting in the loss of rotational symmetry [2–4]. The fluid motion is thus much more difficult to analyze: hence, one can appreciate

the mathematical difficulties encountered in solving the resultant problem.

An excellent survey of literature of combined free and forced convection in vertical tubes is given in the work of Hallman [5], and Ojalvo and Grosh [6]. For a historical review of the general problem of mixed convection, the reader is referred to Metais [1]. Recent experimental work in this area was reported by Mori *et al.* [2], Shannon and Depew [7], McCamas and Eckert [8], and Eckert and Peterson [9]. On the other hand, the latest theoretical attempts were by Morton [3], Iqbal and Stachiewicz [4], and Mori *et al.* [10]. An up to date survey of combined free and forced convection in a horizontal tube is given by Faris [11].

While many aspects of the physical nature of the combined phenomena remain uncertain, this much has been established:

(a) In general free convection effects are more pronounced for low Prandtl number fluids than for high ones.
(b) There are no appreciable free convection effects in the thermal entrance region.
(c) For a uniform wall heat flux boundary condition, fully developed heat transfer is reached asymptotically after a considerable starting length [2, 7]. For example, $Z/D > 700$ was needed to establish fully developed heat transfer for water [7] as compared to $Z/D = 180$ for air [2].
(d) For turbulent flow, buoyancy has little effect on the velocity and temperature fields, liquid metals being excepted.
(e) For constant heat flux boundary conditions and fully developed heat transfer $\partial T/\partial Z = \partial T_m/\partial Z =$ constant.
(f) Both velocity and temperature profiles, while similar to each other, are markedly different from their respective counterparts for pure forced convection.
(g) In the fully developed region, the average Nusselt number [2, 7, 8, 11] is higher than that of pure forced convection.

The problem considered in the present study is one of combined free and forced convection heat transfer for laminar flow inside a horizontal circular tube with a uniform heat flux prescribed at the wall. The primary motivation is to improve our understanding of the combined process and to extend the existing solutions to a wider range of conditions so that the analytical results may find direct physical application. The mathematical model considered herein approximates many engineering problems of practical importance such as heating or cooling of fluids inside channels.

2. ANALYSIS

2.1 *Physical model and simplifying assumptions*

For the geometry depicted in Fig. 1, the natural choice is a cylindrical coordinate system with the position denoted by the coordinates r, ϕ, and Z. The problem considered here is one of combined free and forced convection

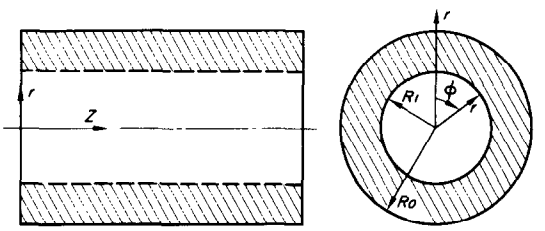

FIG. 1. Schematic diagram and coordinate system.

in a horizontal circular tube. The flow is considered to be steady and laminar. In addition, temperature and velocity profiles in the fluid are assumed fully developed, a condition that has been discussed in detail elsewhere [11]. The solutions are expected to be valid only at distances far enough from entrance and exit of the tube where both the velocity and temperature profiles are invariant with the axial coordinate at each cross section, that is, in the fully developed flow and heat transfer region. All physical properties are considered to be independent of temperature. The density is temperature dependent only in the buoyancy

term. Furthermore, the axial pressure gradient is considered constant. This assumption is valid except for very low Reynolds numbers [8], that is, when $Re_D^2 \ll 650$. The boundary condition imposed on the tube wall is that of uniform heat flux along the tube and around the circumference. In addition, the inside tube wall temperature is assumed constant along the periphery but varies linearly downstream [11].

2.2 *Discussion of the assumptions*

Because of differences in density resulting from the temperature differences between the tube wall and the fluid, the effects of buoyancy are superimposed on the fluid motion along the tube axis as a consequence of external pressure forces. The secondary flow, produced by these buoyancy forces, distorts the Poiseullian velocity distribution to a form of helical motion [10]. The body force term in the momentum equations gives rise to the circulation of the fluid within the tube which results in a non-uniform circumferential inside tube wall temperature. However, as shown in detail elsewhere [11], the angular variation of the wall temperature can be neglected for most physical situations of practical interest.

As a consequence of the secondary flow produced by the buoyancy forces, there are present in the fluid tangential and radial velocity components. Far downstream from hydrodynamic and thermal entrance regions the velocity components resulting from the constant temperature difference between the tube wall and the bulk fluid [2–4] will eventually become independent of the axial distance. The present analysis is confined to this region of the flow commonly referred to as the fully developed region.

2.3 *The governing equations*

Subject to the assumptions made previously, the conservation equations written in cylindrical coordinates reduce to:

Conservation of mass.

$$\frac{\partial U}{\partial r} + \frac{U}{r} + \frac{1}{r}\frac{\partial V}{\partial \phi} = 0 \tag{1}$$

Conservation of momentum.

r-direction

$$\rho\left[U\frac{\partial U}{\partial r} + \frac{V}{r}\frac{\partial U}{\partial \phi} - \frac{V^2}{r}\right] = -\frac{\partial P}{\partial r} + \mu\left[\nabla^2 U - \frac{U}{r^2} - \frac{2}{r^2}\frac{\partial V}{\partial \phi}\right] + \rho g_r \tag{2}$$

ϕ-direction

$$\rho\left[U\frac{\partial V}{\partial r} + \frac{V}{r}\frac{\partial V}{\partial \phi} + \frac{UV}{r}\right] = -\frac{1}{r}\frac{\partial P}{\partial \phi} + \mu\left[\nabla^2 V - \frac{V}{r^2} + \frac{2}{r^2} + \frac{\partial U}{\partial \phi}\right] + \rho g_\phi \tag{3}$$

Z-direction

$$\rho\left[U\frac{\partial W}{\partial r} + \frac{V}{r}\frac{\partial W}{\partial \phi}\right] = -\frac{\partial P}{\partial Z} + \mu\nabla^2 W + \rho g_z \tag{4}$$

Conservation of energy.

$$\rho c_p\left[U\frac{\partial T}{\partial r} + \frac{V}{r}\frac{\partial T}{\partial \phi} + W\frac{\partial T}{\partial Z}\right] = k\left[\nabla^2 T + \frac{\partial^2 T}{\partial Z^2}\right] + \mu\Phi. \tag{5}$$

The boundary conditions for the preceding equations are arrived at from the assumption of a no-slip condition of the velocity at the tube wall, from the finiteness of the flow and temperature at the tube axis, and from the specification of thermal boundary conditions at the tube wall. Consequently,

$$U, V, W, T \text{ are finite at } r = 0 \tag{6}$$

and

$$\left.\begin{aligned} U = V = W = 0 \\ -k\left.\frac{\partial T}{\partial r}\right|_{r=R_i} = q_w'' \end{aligned}\right\} \text{ at } r = R_i. \tag{7}$$

It should be noted that the foregoing system of equations is nonlinear, nonhomogeneous, and coupled. Understandably then, they are not amenable to a closed form solution. Furthermore, no formal procedure for solving the general problem is available, nor does one appear imminent; hence, various simplifying approximations have been introduced in order to make the physical problem more tractable mathematically. Consequently, one must resort to approximate methods of solution, namely, finite difference approximations or perturbation techniques.

In principle, an approximate finite-difference solution can be found for a system of partial differential equations which will converge to the exact analytical solution; however, it is not generally true that all finite difference schemes will readily converge. If convergence is not achieved, the system is said to be unstable [12]. Unfortunately, the stability criteria can rarely be determined a priori, especially for a nonlinear system of equations such as the one at hand. Since the primary objective of this study is to obtain a qualitative understanding of the phenomena, it was felt desirable to obtain a closed form approximate analytical solution. Therefore, finite difference technique for solving the conservation equations was not considered. As will be shown later after a few key assumptions it is possible to arrive at an approximate closed form solution.

2.4 *Reduction of the governing equations*

A question of primary importance is the definition of characteristic tangential and radial velocities for the combined free and forced convection heat transfer. For this problem there is no unique characteristic velocity that can be determined a priori. Obviously, the radial and tangential velocities are not of the same order of magnitude as the axial velocity, and hence they cannot all be normalized by a single reference velocity, say, the mean velocity or the centerline velocity as was done previously [3, 4]. Thus, a characteristic velocity must be determined from the differential equations.

Moreover, since the radial and tangential velocity components are due to the buoyancy force in the fluid, then a parameter depicting the temperature distribution in the fluid must be introduced in the dimensionalization scheme. With this in mind, it was felt that the velocity components should be normalized as follows:

$$u = U/\varepsilon A; \quad v = V/\varepsilon A; \quad w = W/W_m \tag{8}$$

where $\varepsilon = \beta(T_w - T_m)$ and β is the thermal expansion coefficient and A is a characteristic velocity to be determined later. The introduction of such a reference velocity was first suggested by Ostrach [13] in his analysis of a pure free convection problem. It is felt that Ostrach's approach is also applicable in the present combined free and forced convection problem.

In order to obtain explicit dimensionless parameters, the characteristic velocity A must be determined. This may be deduced from the momentum equation. Thus, depending on the type of the flow under consideration, the buoyancy force may be equated to either the viscous or the inertia force to yield A. For example, if the flow is such that the buoyancy and inertia forces are of the same order of magnitude, equating them yields [11]

$$A = \sqrt{\left(\frac{gR_i}{\varepsilon}\right)} = \sqrt{\left(\frac{gR_i}{\beta(T_w - T_m)}\right)}. \tag{9}$$

By introducing the dimensionless variables defined below

$$\eta = r/R_i; \quad z = Z/L; \quad p = P/\rho W_m^2;$$

$$\theta = (T_w - T)/(T_w - T_m)$$

one can show that equations (1)–(5) reduce to the following:

Conservation of mass.

$$\frac{\partial u}{\partial \eta} + \frac{u}{\eta} + \frac{1}{\eta}\frac{\partial v}{\partial \phi} = 0. \tag{10}$$

Conservation of momentum.

r-direction

$$\frac{Gr}{Re^2}\left[u\frac{\partial u}{\partial \eta}+\frac{v}{\eta}\frac{\partial u}{\partial \phi}-\frac{v^2}{\eta}\right]=-\frac{\partial p}{\partial \eta}+\frac{Gr}{Re^2\sqrt{Gr}}\left[\frac{\partial}{\partial \eta}\left(\frac{1}{\eta}\frac{\partial}{\partial \eta}(\eta u)\right)+\frac{1}{\eta^2}\frac{\partial^2 u}{\partial \phi^2}-\frac{2}{\eta^2}\frac{\partial v}{\partial \phi}\right]-\frac{Gr}{Re^2}\theta\cos\phi. \quad (11)$$

ϕ-direction

$$\frac{Gr}{Re^2}\left[u\frac{\partial v}{\partial \eta}+\frac{v}{\eta}\frac{\partial v}{\partial \phi}+\frac{uv}{\eta}\right]=-\frac{1}{\eta}\frac{\partial p}{\partial \phi}+\frac{Gr}{Re^2\sqrt{Gr}}\left[\frac{\partial}{\partial \eta}\left(\frac{1}{\eta}\frac{\partial}{\partial \eta}(\eta v)\right)+\frac{1}{\eta^2}\frac{\partial^2 v}{\partial \phi^2}+\frac{2}{\eta^2}\frac{\partial u}{\partial \phi}\right]+\frac{Gr}{Re^2}\theta\sin\phi. \quad (12)$$

Z-direction

$$u\frac{\partial w}{\partial \eta}+\frac{v}{\eta}\frac{\partial w}{\partial \phi}=-\frac{\gamma}{\sqrt{Gr}}+\frac{1}{\sqrt{Gr}}\left[\frac{1}{\eta}\frac{\partial}{\partial \eta}\left(\eta\frac{\partial w}{\partial \eta}\right)+\frac{1}{\eta^2}\frac{\partial^2 w}{\partial \phi^2}\right]. \quad (13)$$

Conservation of energy.

$$u\frac{\partial \theta}{\partial \eta}+\frac{v}{\eta}\frac{\partial \theta}{\partial \phi}-\left(\frac{Gr_Z}{Gr}\right)\frac{Re}{\sqrt{Gr}}w=\frac{1}{Pr\sqrt{Gr}}\left[\frac{1}{\eta}\frac{\partial}{\partial \eta}\left(\eta\frac{\partial \theta}{\partial \eta}\right)+\frac{1}{\eta^2}\frac{\partial^2 \theta}{\partial \phi^2}+\left(\frac{R_i}{L}\right)^2\frac{\partial^2 \theta}{\partial z^2}\right]+\frac{F}{\sqrt{Gr}}\Phi^+ \quad (14)$$

The boundary conditions in dimensionless form for the preceding equations are:

$$w, \theta, v, u \text{ are finite at } \eta = 0 \quad (15)$$

and

$$w = \theta = v = u = 0 \text{ at } \eta = 1 \quad (16)$$

2.5 *Solution of the governing equations*

The continuity equation is identically satisfied by introducing the stream function ψ defined as

$$\frac{1}{\eta}\frac{\partial \psi}{\partial \phi} = v \quad \text{and} \quad -\frac{\partial \psi}{\partial \eta} = v. \quad (17)$$

After writing equations (11) and (12) in terms of ψ, the pressure gradient can be eliminated between the two equations by cross differentiation and subtraction yielding

$$\frac{\sqrt{Gr}}{Re^2}\nabla^4\psi+\frac{1}{\eta}\frac{Gr}{Re^2}\left[\frac{\partial \psi}{\partial \eta}\frac{\partial}{\partial \phi}-\frac{\partial \psi}{\partial \phi}\frac{\partial}{\partial \eta}\right]\nabla^2\psi+\frac{1}{\eta^4}\frac{\partial \psi}{\partial \phi}\left[2\frac{\partial^2 \psi}{\partial \phi^2}+\eta\frac{\partial \psi}{\partial \eta}\right]\frac{Gr}{Re^2}=\frac{Gr}{Re^2}\left[\frac{1}{\eta}\cos\phi\frac{\partial \theta}{\partial \phi}+\sin\phi\frac{\partial \theta}{\partial \eta}\right]. \quad (18)$$

From the definition of ψ, as given by equation (17), it can be seen that the Z-component of the momentum equation can be written as

$$\nabla^2 w+\frac{\sqrt{Gr}}{\eta}\left[\frac{\partial \psi}{\partial \eta}\frac{\partial}{\partial \phi}-\frac{\partial \psi}{\partial \phi}\frac{\partial}{\partial \eta}\right]w-\gamma=0. \quad (19)$$

Similarly, the energy equation (14) becomes

$$\nabla^2\theta+\frac{Pr\sqrt{Gr}}{\eta}\left[\frac{\partial \psi}{\partial \eta}\frac{\partial}{\partial \phi}-\frac{\partial \psi}{\partial \phi}\frac{\partial}{\partial \eta}\right]\theta+\frac{Gr_Z Re}{Gr^{\frac{3}{2}}}w=0. \quad (20)$$

The viscous dissipation and axial heat conduction terms have been neglected since it has been shown [11] that these terms are negligible in comparison with the others in the conservation of energy equation.

The boundary conditions in dimensionless form for the said equations are

$$w, \theta, \frac{1}{\eta}\frac{\partial \psi}{\partial \phi}, \frac{\partial \psi}{\partial \eta} \text{ are finite at } \eta = 0 \quad (21)$$

and

$$w = \theta = \frac{\partial \psi}{\partial \phi} = \frac{\partial \psi}{\partial \eta} = 0 \quad \text{at} \quad \eta = 1. \quad (22)$$

An examination of equations (18)–(20) together with the prescribed boundary conditions reveals that a closed form solution appears to be improbable, if not impossible. Thus, in the absence of any exact solution for the dependent variables ψ, w, and θ these variables are expanded in a power series in ascending order of Gr/Re^2.

The power series expansion of the dependent variables is taken of the form [15]

$$\psi = \psi_0 + \left(\frac{Gr}{Re^2}\right)\psi_1 + \left(\frac{Gr}{Re^2}\right)^2 \psi_2 + \dots \quad (23)$$

$$w = w_0 + \left(\frac{Gr}{Re^2}\right) w_1 + \left(\frac{Gr}{Re^2}\right)^2 w_2 + \dots \quad (24)$$

$$\theta = \theta_0 + \left(\frac{Gr}{Re^2}\right)\theta_1 + \left(\frac{Gr}{Re^2}\right)^2 \theta_2 + \dots . \quad (25)$$

For pure forced convection, $Gr = 0$, no circulation exists so that $\psi_0 = 0$. However, the evaluation of the remaining dependent variables is more involved since it requires the substitution of equations (23)–(25) in equations (18)–(20) and the terms of like powers of Gr/Re^2 grouped together. Taking terms up to the second order in the perturbation parameter Gr/Re^2 the following three sets of partial differential equations result.

Zero order approximation:

$$\nabla^2 w_0 - \gamma = 0 \quad (26a)$$

$$\nabla^2 \theta_0 + \frac{PeGr_z}{Gr} w_0 = 0. \quad (26b)$$

First order approximation:

$$\nabla^4 \psi_1 = \frac{Re^2}{\sqrt{(GrRe)}}\left[\frac{1}{\eta}\frac{\partial \theta_0}{\partial \phi}\cos\phi + \frac{\partial \theta_0}{\partial \eta}\sin\phi\right] \quad (27a)$$

$$\nabla^2 w_1 + \frac{\sqrt{Gr}}{\eta}\left[\frac{\partial \psi_1}{\partial \eta}\frac{\partial w_0}{\partial \phi} - \frac{\partial \psi_1}{\partial \phi}\frac{\partial w_0}{\partial \eta}\right] = 0 \quad (27b)$$

$$\nabla^2 \theta_1 + \frac{Pr\sqrt{Gr}}{\eta}\left[\frac{\partial \psi_1}{\partial \eta}\frac{\partial \theta_0}{\partial \phi} - \frac{\partial \psi_1}{\partial \phi}\frac{\partial \theta_0}{\partial \eta}\right] + \frac{PeGr_z}{Gr} w_1 = 0. \quad (27c)$$

Second order approximation:

$$\nabla^4 \psi_2 = \frac{Re}{\sqrt{(ReGr)}}\left[\frac{1}{\eta}\frac{\partial \theta_1}{\partial \phi}\cos\phi + \frac{\partial \theta_1}{\partial \eta}\sin\phi\right] \quad (28a)$$

$$\nabla^2 w_2 + \frac{\sqrt{Gr}}{\eta}\left[\frac{\partial \psi_2}{\partial \eta}\frac{\partial w_0}{\partial \phi} + \frac{\partial \psi_1}{\partial \eta}\frac{\partial w_1}{\partial \phi}\right] = \frac{\sqrt{Gr}}{\eta}\left[\frac{\partial \psi_2}{\partial \phi}\frac{\partial w_0}{\partial \eta} + \frac{\partial \psi_1}{\partial \phi}\frac{\partial w_1}{\partial \eta}\right] \quad (28b)$$

$$\nabla^2 \theta_2 + \frac{Pr\sqrt{Gr}}{\eta}\left[\frac{\partial \psi_2}{\partial \eta}\frac{\partial \theta_0}{\partial \phi} + \frac{\partial \psi_1}{\partial \eta}\frac{\partial \theta_1}{\partial \phi}\right] = \frac{Pr\sqrt{Gr}}{\eta}\left[\frac{\partial \psi_2}{\partial \phi}\frac{\partial \theta_0}{\partial \eta} + \frac{\partial \psi_1}{\partial \phi}\frac{\partial \theta_1}{\partial \eta}\right] - \frac{PrGr_z}{Gr} w_2 \quad (28c)$$

The general boundary conditions which are essential to the complete specification of the solution of the preceding equations are essentially equivalent to those given by equations (21) and (22).

The method used in solving the preceding equations may be divided into two distinct parts. First, the partial differential equations are transformed into ordinary differential equations by assuming a form of solution which, in addition to eliminating one of the independent variables and satisfying the imposed boundary conditions, is physically justified from the data of Mori *et al.* [2] and was successfully employed by Morton [3]. Second, the resulting ordinary differential equations are then solved by a novel approach discussed in detail in [11].

Equations (26a) and (26b) are for Poiseuille flow without free convection effects and their solution is available in elementary texts [14]. The remaining equations are solved by substituting the forced-flow solution in the equations of first order in the perturbation parameter Gr/Re^2 and proceeding step by step. It must be noted, however, that the present

perturbation solution applies merely to the case of perturbing free convection effects on a predominantly forced convection flow. The detailed solution of equation (26a)–(28c) is given elsewhere [11]. Since the expressions for ψ, w, and θ are lengthy they are given in Appendix A.

2.6 *Heat transfer*

The local circumferential convective heat transfer coefficient is defined as

$$h(\phi) \equiv \frac{q_i''(\phi)}{(T_w - T_m)} = -\frac{k}{(T_w - T_m)} \frac{\partial T}{\partial r}\bigg|_{r=R_i} \quad (29)$$

where T_m is the mixing cup temperature. In terms of the dimensionless variables, the local (circumferential) heat transfer coefficient becomes

$$h(\phi) = -\frac{k}{R_1} \frac{\partial \theta(\phi)}{\partial \eta}\bigg|_{\eta=1}. \quad (30)$$

The local Nusselt number, $Nu(\phi)$, based on the inside radius of the tube as the characteristic dimension is defined as

$$Nu(\phi) \equiv \frac{h(\phi)R_i}{k} = -\frac{\partial \theta(\phi)}{\partial \eta}\bigg|_{\eta=1}. \quad (31)$$

Finally, substituting equation (A.3) in equation (31) and simplifying gives the ratio of the local Nusselt number to the Nusselt number for pure forced convection as

$$\frac{Nu(\phi)}{Nu_0} = 1{\cdot}0 - \Gamma[0{\cdot}277 \times 10^{-3} Pr + 0{\cdot}104 \times 10^{-3}] \cos\phi + \Gamma^2[2{\cdot}175 \times 10^{-8} Pr^2 + 1{\cdot}0025 \times 10^{-7} Pr] + \Gamma^2[0{\cdot}688 \times 10^{-8} Pr^2 + 0{\cdot}06 \times 10^{-6} Pr - 0{\cdot}833 \times 10^{-7}] \cos 2\phi \quad (32)$$

where Nu_0 is the Nusselt number for pure forced convection.

The average heat transfer coefficient $\bar{h}$ is defined as

$$\bar{h} = \frac{1}{2\pi} \int_0^{2\pi} h(\phi)\, d\phi. \quad (33)$$

If the indicated integration is performed and an average Nusselt number $\overline{Nu}$ is introduced, there results

$$\frac{\overline{Nu}}{Nu_0} = 1{\cdot}0 + \Gamma^2[2{\cdot}175 \times 10^{-8} Pr^2 + 1{\cdot}0025 \times 10^{-7} Pr]. \quad (34)$$

3. RESULTS AND DISCUSSION

3.1 *A check on the validity and accuracy of the perturbation solutions*

In view of the fact that no exact solutions exist, a knowledge of the range of the validity of the present perturbation method is of considerable importance. Equations (A.1)–(A.3) indicate that the three velocity components as well as the temperature distributions at any cross section of the tube are functions of Grashof, Prandtl, and Reynolds numbers. In order to examine the limitations of the solutions of these equations, numerical calculations were performed to study their convergence for various combinations of the governing parameters. More specifically, the critical radii η_c corresponding to, say, the maximum axial velocities (w_0, w_{0+1}, w_{0+1+2}) were determined from the said equations for a fixed Prandtl number and for different values of the parameter Γ. The comparison at the critical radii was then made of the successive approximations of the axial velocities, i.e.,

$$(w_{0+1+2} - w_{0+1}) \leqslant (w_{0+1} - w_0).$$

This procedure was repeated for different Prandtl numbers, and thus the limits of convergence were established. A similar procedure was followed for the temperature and the average Nusselt numbers [11]. The analysis showed that the limits of convergence for the axial velocity, temperature, and average Nusselt numbers may be considerably different [11]. This also appears to be the case in the analysis of Morton [3] and Iqbal and Stachiewicz [4] and may be attributed to the fact that the velocity is less sensitive to the variation in the parameter

Γ and the Prandtl number Pr than the temperature and average Nusselt number $\overline{Nu}$.

A detailed check of Morton's [3] results indicates that his equation for the Nusselt number is convergent in a region where the temperature equation is divergent [4], and therefore, his results are questionable in this range. On the other hand, a check of Iqbal and Stachiewicz's [4] results reveals that the upper limit for the temperature and the Nusselt number equations for air is at $ReRa = 1500$ as compared to $ReRa \simeq 3000\sqrt{Re}$ for the present analysis. This prohibits any comparison between their theoretical results and available experimental data.

3.2 *Comparison of available experimental data with theoretical predictions*

The analytical predictions of this study are compared with other theoretical investigations and experimental data in Figs. 2 and 3. A comparison is given of the present analysis with

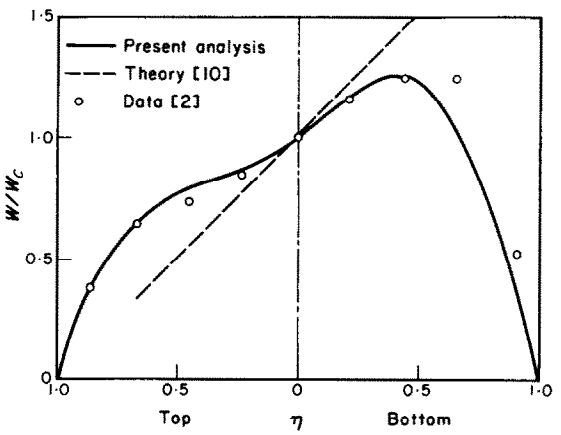

FIG. 2. Comparison of axial velocity profiles between present analysis and other theoretical and experimental investigations for air at $\Gamma = 1200$ and $Pr = 0{\cdot}72$.

the theory and experiment of Mori *et al.* [2, 10] for velocity and temperature distributions in the vertical plane. A reasonably good agreement is demonstrated between the present analysis and the experimental data of Mori *et al.* [2]. The correlation between the theoretical analysis of Mori *et al.* [10] and their own data [2] is quite poor. It should be noted that in both the velocity and temperature profiles there is some discrepancy between the present predictions and the experimental data [2] at the bottom of the tube. As will be shown later in this region the vorticity is maximum. It is felt that the poorer agreement in this region may be attributed to the presence of turbulent flow which is not accounted for in this work. Furthermore, it can be concluded from both figures that in the

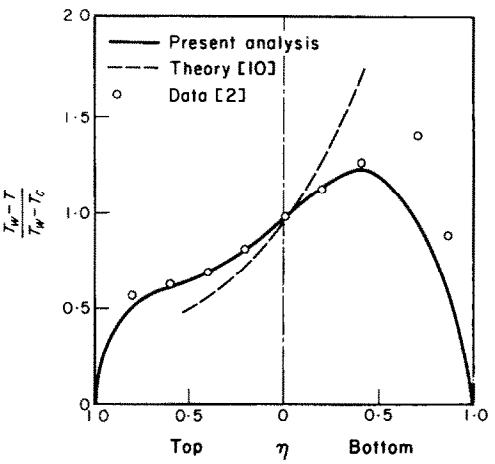

FIG. 3. Comparison of temperature profiles in the vertical plane between present analysis and other theoretical and experimental investigations for air at $\Gamma = 1200$ and $Pr = 0{\cdot}72$.

vicinity of the tube wall both the velocity and temperature change abruptly, a trend which has been observed previously [2–4]. On the other hand, in the core the variation of both velocity and temperature with the radius is essentially linear.

3.3 *Prediction of the flow pattern and isotherms*

A more complete understanding of the flow characteristics may be gained by observing the flow field. As an illustration of the streamline pattern for the heating of air at $\Gamma = 1200$ is shown in Fig. 4. This particular value of Γ was chosen so that present results correspond to

the experimental data of Mori *et al.* [2]. In order to provide a more complete description of the combined phenomena for any one particular case these same values of the parameters shall be used in illustrating other aspects of the solutions. It can be seen from Fig. 4 that there exist two cells of the crescent-eddy type symmetrical about the vertical plane ($\phi = 0$). This type of flow pattern has been photographed and discussed by Mori *et al.* [10]. For heating, the wall temperature is higher than the fluid temperature, and thus the fluid near the wall, being hotter than that in the core, ascends near the wall toward the top.

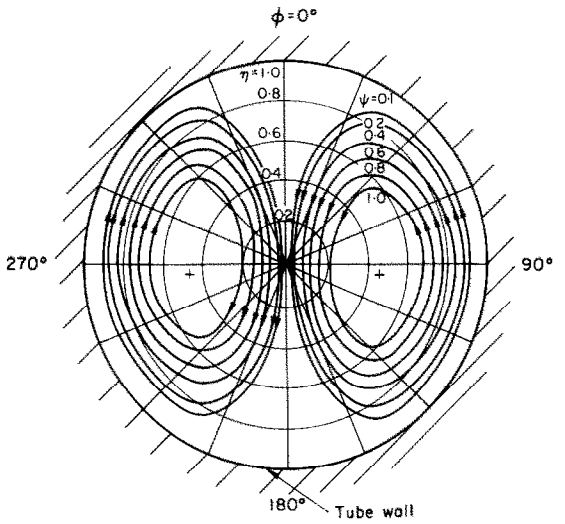

FIG. 4. Streamline pattern for air at $\Gamma = 1200$ and $Pr = 0{\cdot}72$.

The two upward flows along both sides of the tube wall meet at the upper part of the tube, $\phi = 0$, change direction, and descend in the central portion as the fluid moves through the tube.

By defining the center of the eddy to be the point where ψ has its maximum value it can be shown that the center is located at $\eta = 0{\cdot}46$ and $\phi = 95$ and 265 for the parameters of Fig. 4. The location of the center of the eddy depends on the Prandtl number Pr and the parameter Γ.

Figure 5 depicts the constant axial velocity lines for air at $\Gamma = 1200$. The concentration of the constant axial velocity lines in the vicinity of $\phi = \pi$ indicates high velocity gradients and thus a high degree of vorticity and a large shear stress. The constant radial and tangential velocity lines are presented in Figs. 6 and 7

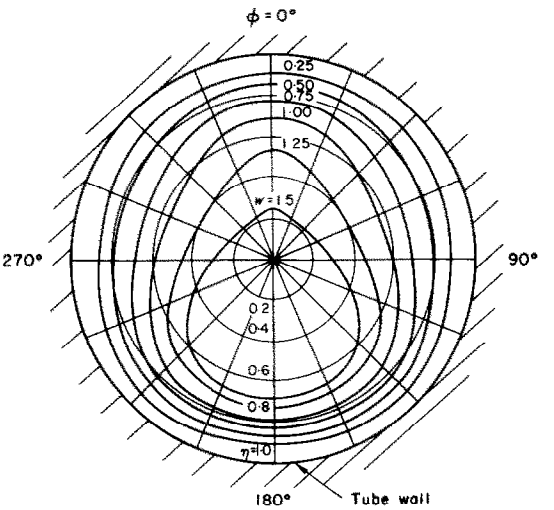

FIG. 5. Constant axial velocity lines for air at $\Gamma = 1200$ and $Pr = 0{\cdot}72$.

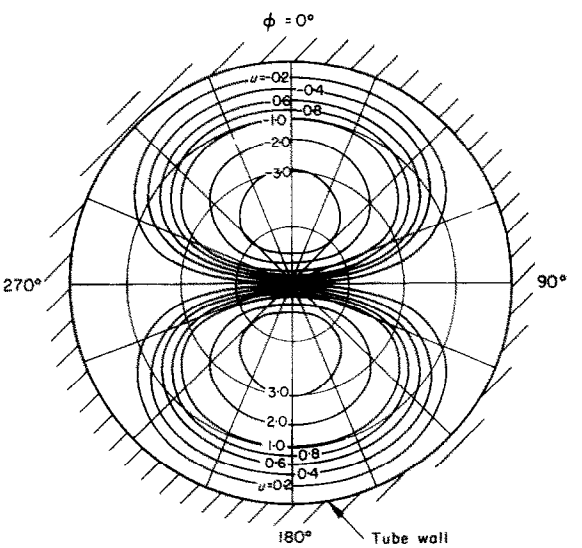

FIG. 6. Constant radial velocity lines for air at $\Gamma = 1200$ and $Pr = 0{\cdot}72$.

respectively. The radial velocity pattern depicted in Fig. 6 reveals that the velocity is antisymmetric about the horizontal plane ($\phi = \pi/2$). The radial velocity increases as the center is approached, and the change in sign results merely from the mathematical definition. This is consistent with the results presented in Fig. 4.

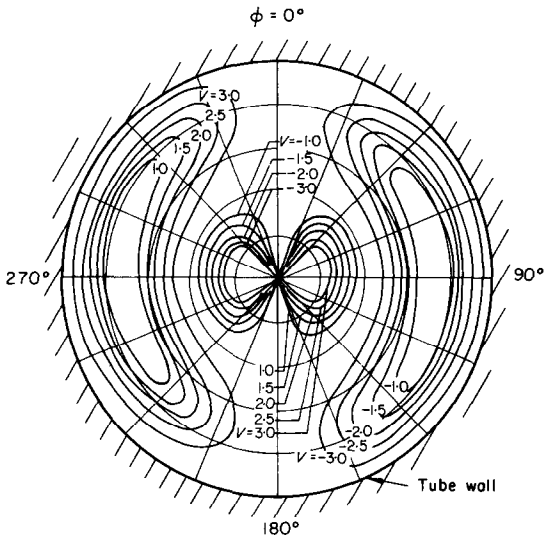

FIG. 7. Constant tangential velocity lines for air at $\Gamma = 1200$ and $Pr = 0{\cdot}72$.

The effects of the buoyancy force is particularly evident in Fig. 7 where the constant tangential velocity lines are shown. Recall that v is positive in the positive ϕ direction. A close inspection of Fig. 7 reveals that the tangential velocity component is upwards in the vicinity of the tube wall and downward in the core region. This is in accordance with physical reasoning for heating of the fluid and may also be deduced from the streamline pattern of Fig. 4. Again, the change in the sign of the tangential velocity component results merely from the mathematical definition.

The isotherms are presented in Fig. 8 for air at $\Gamma = 1200$. The region of the maximum temperature gradients and thus maximum heat transfer occurs at $\phi = \pi$ where the isotherms are concentrated.

An illustration of the effect of the parameter Γ on the axial velocity and temperature profiles

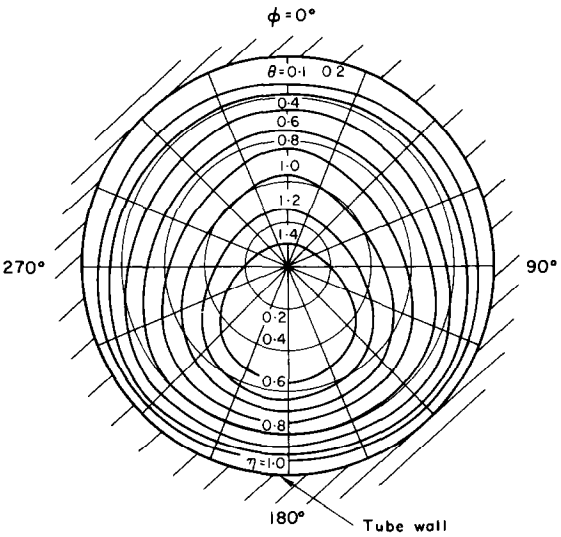

FIG. 8. Isotherms for air at $\Gamma = 1200$ and $Pr = 0{\cdot}72$.

for air in the vertical plane are shown in Figs. 9 and 10, respectively. For $\Gamma = 0$ the buoyancy forces are absent and hence the problem reduces to a pure forced convection one as depicted by the solid line in both figures. As

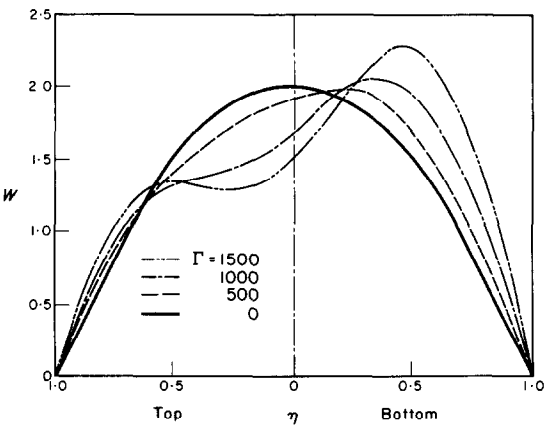

FIG. 9. Effect of the parameter Γ on the axial velocity profile in the vertical plane for air at $Pr = 0{\cdot}72$.

Γ increases, the free convection effects become more pronounced. The secondary flow increases correspondingly and both the axial velocity and temperature profiles become distinctly different from those of pure forced convection. Furthermore, due to the secondary flows, both the velocity and temperature distributions exhibit a minima in the upper half of the tube, a trend which has also been observed previously [2–4].

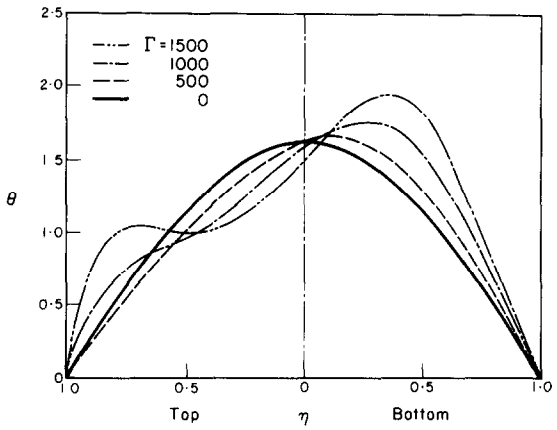

FIG. 10. Effect of the parameter Γ on the temperature profile in the vertical plane for air at $Pr = 0{\cdot}72$.

3.4 *The effect of the Prandtl number and the parameter Γ on average Nusselt numbers*

The effect of the parameter Γ on the Nusselt number ratio $\overline{Nu}/Nu_0$ is shown in Fig. 11 for different Prandtl numbers. The results for fluids with Pr ranging from 0·003 (potassium) to 40·0 (light oil) are presented. The trends are primarily due to the physical nature of the parameter Γ and are similar to those obtained by Mori *et al.* [2, 10]. It should be noted that for air at $\Gamma = 3{\cdot}6 \times 10^3$ the average Nusselt number for combined free and forced convection is twice as high as that for pure forced convection.

Finally, in Fig. 12 a comparison between the present analysis and those of Morton [3] and Iqbal and Stachiewicz [4] as well as the experimental data for air of Mori *et al.* [2] and McComas and Eckert [8] are presented for the average Nusselt number as a function of the parameter Γ.† The present analysis shows good agreement with the experimental results

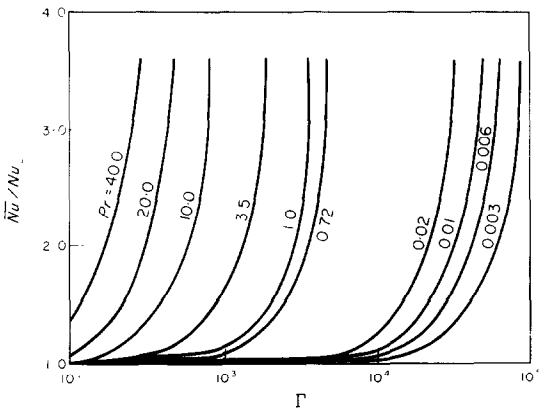

FIG. 11. Dependence of the ratio $\overline{Nu}/Nu_0$ on Γ with the Prandtl number Pr as a parameter.

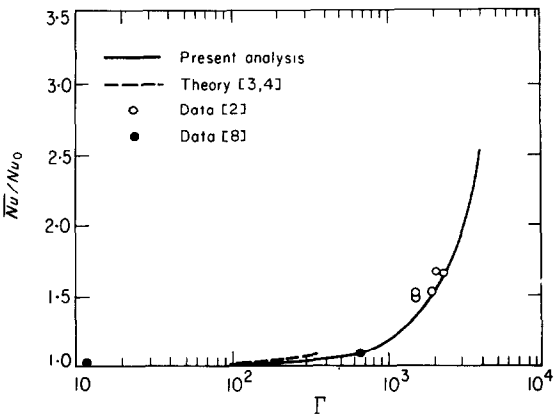

FIG. 12. Comparison of the ratio $Nu(\phi)/Nu_0$ between present analysis and other experimental and theoretical investigations for air at $\Gamma = 1200$ and $Pr = 0{\cdot}72$.

[2, 8]. Moreover, the limitations of the applicability of the theoretical predictions of [3] and [4] are illustrated by the divergence of their series solution at low values of the parameter Γ.

† Only those data points for which sufficient information was given in [2] to transform the parameter $Re\ Ra$ to Γ are included in the figure.

4. CONCLUSION

Results of the analysis have been presented in graphical form. Many restrictive assumptions have been made in the formulation and solution of the problem so that the results obtained have a somewhat qualitative character and must be considered as a first approximation to the real problem. Nevertheless, it can be concluded that:

1. The perturbation method, when properly employed, can be a successful tool in solving the governing differential equations describing the mixed convection phenomena.
2. The velocity and temperature profiles are similar to each other but differ markedly from their respective counterparts for pure forced convection. Furthermore, both the velocity and temperature change noticeably in the vicinity of the tube wall.
3. The average Nusselt number for combined free and forced convection is substantially higher than that of pure forced convection. This is due to secondary flow effects.
4. For all fluids, excepting liquid metals, the assumption that the inside tube wall temperature is independent of the polar angle ϕ is justifiable for ordinary tube thickness in view of the fact that the ratio of the thermal conductivities of the tube wall and the fluid is usually very high. For liquid metals, the dependence of the inside tube wall temperature on the polar angle ϕ, although more pronounced, may still be neglected for moderate variations in the local heat transfer coefficient $h(\phi)$.

ACKNOWLEDGEMENTS

The authors wish to acknowledge Professor E. R. G. Eckert for his interest in this work and for the helpful discussions in interpreting the results. To Professor F. Schultz-Grunow the authors wish to extend their appreciation for reviewing the mathematical formulation and the method of solution of the problem. Gratitude is also expressed to Purdue University for making computer facilities available. One of the authors (G.N.F.) wishes to acknowledge the Lebanese Council of Scientific Research for providing financial support in the form of a scholarship.

REFERENCES

1. B. METAIS, Criteria for mixed convection, Heat Transfer Laboratory, Department of Mechanical Engineering, Technical Report No. 51, University of Minnesota (1961).
2. K. MORI, K. FUTAGAMI, S. TOKUDA and M. NAKAMURA, Forced convective heat transfer in uniformly heated horizontal tubes, (1st report) experimental study on the effect of buoyancy, *Int. J. Heat Mass Transfer* **9**, 453–463 (1966).
3. B. R. MORTON, Laminar convection in uniformly heated pipes at low Rayleigh numbers, *Q. Jl. Mech. Appl. Math.* **12**, 410–422 (1959).
4. M. IQBAL and J. W. STACHIEWICZ, Influence of tube orientation on combined free and forced laminar convection heat transfer, *Trans. Am. Soc. Mech. Engrs* (C), *J. Heat Transfer* **88**, 109–116 (1966); also, Variable density effects in combined free and forced convection in inclined tubes, *Int. J. Heat Mass Transfer* **10**, 1625–1629 (1967).
5. T. M. HALLMAN, Combined forced and free convection in a vertical tube, Ph.D. Thesis, Purdue University (1958).
6. M. S. OJALVO and R. J. GROSH, Combined forced and free turbulent convection in a vertical tube, Argonne National Laboratory Report ANL-6528 (1962).
7. R. L. SHANNON and C. A. DEPEW, Combined free and forced laminar convection in a horizontal tube with uniform heat flux, *Trans. Am. Soc. Mech. Engrs* (C) *J. Heat Transfer* **90**, 353–357 (1968).
8. S. T. MCCOMAS and E. R. G. ECKERT, Heat transfer and pressure drop in laminar flow through a circular tube under continuum and rarefied conditions, *Trans. Am. Soc. Mech. Engrs* (C) *J. Heat Transfer* **88**, 147–153 (1966).
9. E. R. G. ECKERT and D. C. PETERSON, Heat transfer to mercury in laminar flow through a tube with constant heat flux, *Trans. Am. Soc. Mech. Engrs* (C), *J. Heat Transfer* **87**, 419–420 (1965).
10. Y. MORI and K. FUTAGAMI, Forced convection heat transfer in uniformly heated horizontal tubes, *Int. J. Heat Mass Transfer* **10**, 1801–1813 (1967).
11. G. N. FARIS, An analytical study of combined free and forced convection in a horizontal tube, Ph.D. Thesis, Purdue University (1968).
12. D. R. HARTREE, *Numerical Analysis*. Oxford University Press, London (1952).
13. S. OSTRACH, New aspects of natural convection heat transfer, *Trans. Am. Soc. Mech. Engrs* **75**, 1287–1290 (1953).
14. J. P. HOLMAN, *Heat Transfer*, p. 120. McGraw-Hill, New York (1963).
15. R. BELLMAN, *Perturbation Techniques in Mathematics, Physics and Engineering*. Holt, Rinehart and Winston, New York (1964).

APPENDIX A

The details of the solution of the system of equations (26a)–(28c) are given elsewhere [11]. For the sake of brevity, only the final expressions for ψ, w, and θ are given below.

The dimensionless stream function:

$$\begin{aligned}\psi = {} & 4{\cdot}3 \times 10^{-4}\,\Gamma[-10\eta + 21\eta^3 - 12\eta^5 + \eta^7]\sin\phi \\ & + 0{\cdot}905 \times 10^{-9}\,\Gamma^2[(0{\cdot}00371\,Pr + 0{\cdot}000371)\,\eta^{14} \\ & - (0{\cdot}125\,Pr + 0{\cdot}01765)\,\eta^{12} + (1{\cdot}172\,Pr + 0{\cdot}182)\,\eta^{10} \\ & - (5{\cdot}42\,Pr + 1{\cdot}04)\,\eta^8 + (15{\cdot}6\,Pr + 2{\cdot}82)\,\eta^6 - (340\,Pr + 93)\,\eta^4 \\ & + (327{\cdot}8\,Pr + 90{\cdot}75)\,\eta^2]\sin 2\phi. \end{aligned} \tag{A.1}$$

The dimensionless velocity in axial direction:

$$\begin{aligned} w = {} & 2(1 - \eta^2) + 0{\cdot}22 \times 10^{-4}\,\Gamma(-\eta^9 + 20\eta^7 - 70\eta^5 + 100\eta^3 - 49\eta)\cos\phi \\ & + 0{\cdot}94 \times 10^{-8}\,\Gamma^2(-24{\cdot}314 + 122{\cdot}5\eta^2 - 254\eta^4 + 282{\cdot}5\eta^6 - 182{\cdot}5\eta^8 \\ & + 68{\cdot}5\eta^{10} - 13{\cdot}8\eta^{12} + 1{\cdot}145\eta^{14} - 0{\cdot}0313\eta^{16}) \\ & + \{0{\cdot}94 \times 10^{-8}\,\Gamma^2(-2{\cdot}908\eta^2 + 2{\cdot}42\eta^4 + 7\eta^6 - 12{\cdot}05\eta^8 + 7{\cdot}08\eta^{10} \\ & - 1{\cdot}663\eta^{12} + 0{\cdot}125\eta^{14} - 0{\cdot}00397\eta^{16}) \\ & - 0{\cdot}181 \times 10^{-7}\,\Gamma^2[(0{\cdot}000059\,Pr + 0{\cdot}000059)\eta^{16} \\ & + (0{\cdot}0026\,Pr + 0{\cdot}000366)\eta^{14} + (0{\cdot}0335\,Pr + 0{\cdot}0052)\eta^{12} \\ & - (0{\cdot}225\,Pr + 0{\cdot}04325)\eta^{10} + (1{\cdot}0425\,Pr + 0{\cdot}1884)\eta^8 \\ & - (42{\cdot}5\,Pr + 11{\cdot}6)\eta^6 + (109\,Pr + 30{\cdot}3)\eta^4 \quad - (67{\cdot}35\,Pr + 18{\cdot}85)\eta^2]\}\cos 2\phi \end{aligned} \tag{A.2}$$

The dimensionless temperature:

$$\begin{aligned}\theta = {} & 0{\cdot}125(\eta^4 - 4\eta^2 + 3) + 0{\cdot}181 \times 10^{-6}\,\Gamma\{(10\,Pr +)\eta^{11} \\ & - (210\,Pr + 30)\eta^9 + (1125\,Pr + 175)\eta^7 - (2600\,Pr + 500)\eta^5 \\ & + (3000\,Pr + 735)\eta^3 - (1325\,Pr + 381)\eta\}\cos\phi \\ & - 0{\cdot}785 \times 10^{-11}\,Pr\,\Gamma^2[-(0{\cdot}278\,Pr + 0{\cdot}0278)\eta^{18} \\ & + (89{\cdot}4\,Pr + 12)\eta^{16} - (1680\,Pr + 251)\eta^{14} + (7260\,Pr + 1290)\eta^{12} \\ & - (15300\,Pr + 3170)\eta^{10} + (22100\,Pr + 4920)\eta^8 - (24800\,Pr \\ & + 5780)\eta^6 + (16800\,Pr + 4330)\eta^4 - (3320\,Pr + 952)\eta^2 \\ & - (1149{\cdot}122\,Pr + 399{\cdot}577)] - 0{\cdot}94 \times 10^{-8}\,Pr\,\Gamma^2[3{\cdot}24 - 806\eta^2 \\ & + 7{\cdot}65\eta^4 - 705\eta^6 + 5{\cdot}64\eta^8 - 1{\cdot}825\eta^{10} + 0{\cdot}475\eta^{12} \\ & - 0{\cdot}0704\eta^{14} + 0{\cdot}00448\eta^{16} - 0{\cdot}0000966\eta^{18}] \\ & + \{0{\cdot}23 \times 10^{-8}\,Pr\,\Gamma^2[(0{\cdot}0000926\,Pr + 0{\cdot}00000926)\eta^{18} \\ & - (0{\cdot}01224\,Pr + 0{\cdot}001715)\eta^{16} + (0{\cdot}162\,Pr + 0{\cdot}0249)\eta^{14} \\ & - (1{\cdot}13\,Pr + 38{\cdot}3)\eta^8 + (500\,Pr + 137{\cdot}5)\eta^6 \\ & - (436\,Pr + 121)\eta^4 + (73{\cdot}73\,Pr + 21{\cdot}022)\eta^2] \\ & - 0{\cdot}795 \times 10^{-10}\,Pr\,\Gamma^2[-(0{\cdot}0624\,Pr + 0{\cdot}0624)\eta^{18}\end{aligned}$$

$$+ (32{\cdot}3\,Pr + 4{\cdot}55)\eta^{16} - (775\,Pr + 116)\eta^{14} + (3520\,Pr + 625)\eta^{12}$$
$$- (5800\,Pr + 1200)\eta^{10} + (4830\,Pr + 1075)\eta^{8} + (865\,Pr + 202)\eta^{6}$$
$$- (3960\,Pr + 1022)\eta^{4} + (1288{\cdot}06\,Pr + 431{\cdot}456)\eta^{2}]$$
$$- 0{\cdot}47 \times 10^{-8}\,\Gamma^{2}[0{\cdot}13397\eta^{2} - 0{\cdot}242\eta^{4} + 0{\cdot}0756\eta^{6}$$
$$+ 0{\cdot}1167\eta^{8} - 0{\cdot}125\eta^{10} + 0{\cdot}049\eta^{12} - 0{\cdot}00865\eta^{14}$$
$$+ 0{\cdot}000496\eta^{16} - 0{\cdot}0000124\eta^{18}] + 0{\cdot}905 \times 10^{-7}\,\Gamma^{2}$$
$$\times [(0{\cdot}000000184\,Pr + 0{\cdot}000000184)\eta^{18} - (0{\cdot}0000103\,Pr$$
$$+ 0{\cdot}00000145)\eta^{16} + (0{\cdot}000173\,Pr + 0{\cdot}000027)\eta^{14}$$
$$- (0{\cdot}00161\,Pr + 0{\cdot}000390)\eta^{12} + (0{\cdot}0108\,Pr + 0{\cdot}001955)\eta^{10}$$
$$- (0{\cdot}71\,Pr + 0{\cdot}1935)\eta^{8} + (3{\cdot}41\,Pr + 0{\cdot}945)\eta^{6}$$
$$- (5{\cdot}6\,Pr + 1{\cdot}568)\eta^{4} + (2{\cdot}89\,Pr + 0{\cdot}8148)\eta^{2}]\} \cos 2\phi. \quad \text{(A.3)}$$

Résumé—On présente une analyse du transport de chaleur par convection forcée et naturelle combinée pour un fluide quasi-incompressible s'écoulant laminairement dans un tube horizontal. On suppose que les propriétées physiques sont indépendantes de la température et l'on considère que le flux de chaleur imposé sur la paroi du tube est uniforme le long du tube et tout autour de la circonférence. L'écoulement et le transport de chaleur sont étudiés dans le cas spécial des conditions entièrement développées et les équations aux dérivées partielles qui en résultent sont résolues par une méthode de perturbation. Des solutions analytiques approchées pour la fonction de courant et les distributions des composantes de vitesse et de température aussi bien que les nombres de Nusselt moyens sont présentés graphiquement dans une gamme de nombres de Prandtl et de Grashof d'intérêt pratique. Les vitesses, les températures et les nombres de Nusselt moyens prédits sont comparés avec les résultats expérimentaux disponibles.

Zusammenfassung—Es wird der Wärmeübergang bei Mischkonvektion in einem waagerechten Rohr, in dem ein quasiinkompressibles Fluid laminar strömt, untersucht. Die Stoffwerte werden als unabhängig von der Temperatur angenommen. Die aufgeprägte Wärmestromdichte an der Rohrwand sei gleichmässig entlang und am Umfang des Rohres. Die Strömung und der Wärmeübergang gelten beschränkt für eingelaufene Zustände. Die erhaltene partielle Differentialgleichung wird mit Hilfe von Störfunktionen gelöst. Analytische Näherungslösungen für die Stromfunktion, die Geschwindigkeitskomponenten und die Temperaturverteilung, sowie mittlere Nusselt-Zahlen werden graphisch im physikalisch interessanten Bereich der Prandtl- und Grashof-Zahl dargestellt.

Berechnete Werte für die Geschwindigkeit, die Temperatur und mittlere Nusselt-Zahlen werden mit zur Verfügung stehenden experimentellen Daten verglichen.

Аннотация—Анализируется теплообмен при течении квазинесжимаемой ламинарной жидкости в горизонтальной трубе при совместной свободной и вынужденной конвекции. Предполагают, что физические свойства не зависят от температуры, а также считают, что наложенный на стенку трубы тепловой поток является однородным по длине трубы и по периметру. Гидродинамика и теплообмен рассматриваются для условий полностью развитого течения, а конечные дифференциальные уравнения в частных производных решены методом возмущений. В интервале изменений чисел Прандтля и Грасгофа, представляющих физический интерес, графически представлены приближенные аналитические решения для функции тока, компонент скорости, профиля температуры, а также для средних чисел Нуссельта. Расчетная скорость, температура и средние числа Нуссельта сопоставляются с имеющимися экспериментальными данными.